Article

JOURNAL OF THE CHINESE CHEMICAL SOCIETY

Synthesis and Quantum Chemical Calculation of Benzamide Derivatives Containing Capsaicin and Their Bacteriostatic and Antifouling Properties

Gang Wu, Xiaohui Jiang, Liangmin Yu*, Shuwei Xia and Xiaolin Yu

Key Laboratory of Marine Chemistry Theory and Technology, Ministry of Education, Ocean University of China, Qingdao 266100, P. R. China

(Received: Jan. 28, 2015; Accepted: Aug. 25, 2015; Published Online: Sept. 18, 2015; DOI: 10.1002/jccs.201500037)

Thirteen benzamide derivatives containing capsaicin (BDCCs) have been successfully synthesized via the current method (Friedel-Crafts alkylation reaction). The resultant monomers were characterized by IR, ^{1}H and ^{13}C NMR, elemental analysis and HRMS. Characterization results were in agreement with the proposed structures of the products. Quantum chemistry calculation yielded three parameters, namely, $\Delta\varepsilon_{L\text{-}H}$, HF values (total energy) and dipole that could explain activity, stability and polarity respectively, and the relationship of each parameter with antimicrobial and antifouling performance was also preliminary discussed. The bacteriostatic property of the 13 compounds was evaluated by minimum inhibitory concentration (MIC) and bacteriostatic ring tests. Experimental results indicated that these compounds can inhibit *Staphylococcus aureus* and *Escherichia coli*. The antifouling effectiveness of the novel antifoulants was investigated using panel tests at the eighth harbor, Qingdao. Four-month exposure results were compared. The compounds exhibited better antifouling properties than the blank panel without antifouling coating or the panel with a common coating. However, test panels with the antifouling coatings were covered with trace amounts of algae and *Balanus* because of weakening of antifouling ability over extended periods of time. All results demonstrate that the new compounds synthesized via our method can be applied in environment-friendly antifouling paints.

Keywords: Benzamide derivatives; Capsaicin; Quantum chemistry; Bacterium-inhibition; Antifouling property.

INTRODUCTION

So far, the most successful mean to prevent the growth of fouling organisms is utilizing antifouling paints which are attached on the hulls of boats and other submerged static structures. These paints are applied because accumulation of fouling organisms increases the frictional resistance of a boat moving through water, thereby resulting in lower speed, greater fuel consumption and poorer maneuverability. Moreover, fouling organisms on static structures will reduce stability and conceal structural defects, and consequently cause the safety issues.[1,2]

Considering that antifouling agents are important components of antifouling coatings, tributyltin (TBT)[3] (Fig. 1) systems earned acclaim in the 1970s as the most effective antifoulant ever developed. TBT is highly effective, provides antifouling properties for five or more years, and maintains the smoothness and low resistance of the boat bottom. Antifouling issues appear to be resolved eventually by this coating. However, TBT presents several adverse effects on the environment;[4-7] the coating has been shown to cause maldevelopment, reproductive failure, gender-bending and sterility of various marine species.[8] Furthermore, studies in coastal waters indicate that TBT accumulates in the marine food chain, thereby leading to abnormal growth in various organisms. As the harm posed by TBT to the marine environment and its severe impact on this ecosystem have become better understood, the United Nations (UN) International Maritime Organization (IMO) decided that coatings containing TBT must be eliminated in vessels less than 25 m long by January 1, 2008.[9] Thus, development of a new environment-friendly antifoulant is biodegradable[10] and harmless to humans and non-target organisms is an urgent necessity.

Capsaicin, which is extracted from chili and other pepper fruits and has a pungent odor (Fig. 2), was recently identified as an effective non-toxic antibacterial and antifouling alternative;[11-13] thus, applicability of this compound in relevant applications has exerted increased research attention.

Despite its promising properties, capsaicin extraction

* Corresponding author. Tel: +86 532 66781845; Fax: +86 532 66781845; Email: Yuyan@ouc.edu.cn

Supporting information for this article is available on the www under http://dx.doi.org/10.1002/jccs.201500037

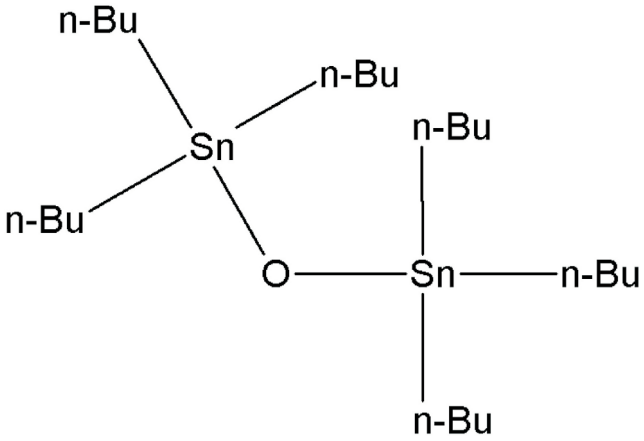

Fig. 1. Structure of TBT.

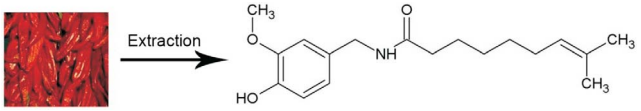

Fig. 2. Structure of capsaicin.

and synthesis are not very feasible because of low yields and high costs, both of which limit its suitability for use as an ideal antifoulant. Recent research has focused on capsaicin analogs, which have been reported to exhibit significant biological activity and are widely used as antifoulants because of their antibacterial and chemical stability properties. This work discusses antifouling paints, with particular emphasis on capsaicin analogs generated by Friedel-Crafts alkylation using an acid as a catalyst;[14,15] this technique can overcome the difficulties of capsaicin extraction. In this study, 13 new capsaicin analogs with good antimicrobial and antifouling properties were obtained. Testing further revealed that the effectiveness of these compounds coincides with their $\Delta\varepsilon_{L\text{-}H}$ and dipoles determined through quantum chemistry calculation.

RESULTS AND DISCUSSION

Quantitative structure and activity relationship

Using Chemoffice software to build compound molecular models, the geometric structures may be optimized by applying density functional theory at the B3LYP/6-31G (d, p) level according to closed shell singlets and preliminarily discussed the relationship of the three parameters ($\Delta\varepsilon_{L\text{-}H}$, HF (total energy) and dipole) and their corresponding activity, stability and polarity. Based on configuration optimization calculations of vibration frequency, the results exhibit no imaginary frequency and determine the stable configurations. We identified the stable structures of the BDCCs and calculated the following parameters: the highest occupied orbital energy (ε_H), the lowest empty orbital energy (ε_L), the difference between the lowest empty and highest occupied orbital energies ($\Delta\varepsilon_{L\text{-}H}$), HF value and dipole. Our findings provide a theoretical basis for further experiments. The calculation results are shown in Table 1.

As can be seen from the contrast of the size of the parameters which were products and the corresponding raw materials, *N*-methylbenzamide grafted on the benzene ring with different functional groups, which exerted a big influence on $\Delta\varepsilon_{L\text{-}H}$, HF and dipole values of the compounds (see Table 1).

The smaller the $\Delta\varepsilon_{L\text{-}H}$, the greater the activity of the compound and the more unstable it is. Results show that the relative stability of the 13 BDCCs follows the order **1f** > **1e** > **1m** > **1b** > **1l** > **1k** > **1a** > **1j** > **1i** > **1h** > **1d** > **1c** > **1g**. For isomers, a lower HF value corresponds to better stability of the compound. The order of **1l** and **1m**, which are isomers is $\mathbf{1m}_{HF} > \mathbf{1l}_{HF}$, so **1l** possesses better stability than **1m**. According to the relationship between the polarity and solvent, the larger the dipole value, the greater the polarity and the easier a compound may be dissolved in a polar solvent. Results show that the polarity of the BDCCs follows the order **1h** > **1j** > **1m** > **1k** > **1e** > **1d** > **1f** > **1b** > **1c** > **1a** > **1g** > **1i** > **1l**.

With regard to $\Delta\varepsilon_{L\text{-}H}$, as can be seen $1(x)_{\Delta\varepsilon L\text{-}H} < 2(x)_{\Delta\varepsilon L\text{-}H}$ (x = b, c, d, e, f, g, h, i, j, k, l, m) from the Table 1, except **1a** > **2a**, the reactivity of the products is superior to those of the raw materials. For **1a**, the hydroxyl portion of the compound increases, but this result may be due to *N*-methylbenzamide substitution at the hydrogen of the benzene ring, which weakens the structural activity of the compound overall. The low activity of the BDCCs and their pungent odor indicate excellent performance as antibacterial and antifouling coatings. In regard to HF, $\mathbf{1(x)}_{HF} > \mathbf{2(x)}_{HF}$ (x = a, b, c, d, e, f, g, h, i, j, k, l, m), the energy of the BDCCs are higher than those of the raw materials because the space volume of the products is fairly large, which increases their instability. For dipole, $\mathbf{1(x)}_{dipole} > \mathbf{2(x)}_{dipole}$ (x = b, c, d, e, f, g, h, i, j, k, l, m), larger dipoles correspond to greater polarity. With the exception of **1a** < **2a**, the polarities of the other BDCCs are greater than those of the raw materials. Thus, when the 13 BDCCs are incorporated as antifoulants into paint, they are expected to show good sol-

Table 1. Parameters of monomers containing capsaicin (1x on behalf of 13 BDCCs, 2x on behalf of the corresponding raw materials, x = a, b, c, d, e, f, g, h, i, j, k, l, m)

Compounds	ε_H/eV	ε_L/ eV	$\Delta\varepsilon_{L-H}$/eV	HF/hartree	Dipole/D
1a	-0.23792	-0.06138	0.17654	-1011.33972712	3.7974
2a	-0.23519	-0.05884	0.17635	-572.25945269	4.5386
1b	-0.21085	-0.03094	0.17991	-1061.07286897	4.2572
2b	-0.20978	0.00848	0.21826	-622.00140574	1.9287
1c	-0.19632	-0.03713	0.15919	-1033.97585319	4.1616
2c	-0.19394	-0.03350	0.16044	-594.89841992	1.9410
1d	-0.22992	-0.06977	0.16015	-901.39196612	5.6437
2d	-0.23685	-0.07087	0.16598	-462.31293712	4.0072
1e	-0.22407	-0.03655	0.18752	-974.44416020	6.3830
2e	-0.22899	-0.03905	0.18994	-535.37034951	3.2871
1f	-0.25735	-0.06153	0.19582	-1223.16761018	5.6332
2f	-0.26779	-0.06337	0.20442	-784.08969684	5.2036
1g	-0.20203	-0.04844	0.15359	-943.13291013	3.6328
2g	-0.20829	0.00526	0.20303	-504.06234886	1.2742
1h	-0.22703	-0.06081	0.16622	-2040.49730879	11.7284
2h	-0.23365	-0.03704	0.19661	-1162.32827916	5.6249
1i	-0.20846	-0.03803	0.17043	-1339.45158627	2.9959
2i	-0.21118	0.00700	0.21818	-461.30075280	2.1925
1j	-0.22171	-0.05009	0.17162	-1380.79441123	8.0892
2j	-0.23137	-0.00269	0.22868	-502.63401022	0.0962
1k	-0.23551	-0.05844	0.17707	-1298.96616820	6.9535
2k	-0.23905	-0.05341	0.18564	-420.80528750	4.5376
1l	-0.21352	-0.03620	0.17732	-1264.25573296	2.7733
2l	-0.21212	0.00815	0.22027	-386.10396522	0.9680
1m	-0.21772	-0.03144	0.18628	-1264.27263405	7.1437
2m	-0.21090	0.00712	0.21802	-386.11939514	1.3606

ubility in the solvent. As such, obtaining more uniform and effective antifouling paints is feasible.

Equilibrium configuration

Compound is obtained by calculating the most stable structure, and their spatial configurations as shown in Fig. 3, the gray on behalf of the C atom, white represents H atom, red represents O atom, blue represents N atom, yellow represents S atom.

Evaluation of antimicrobial activity of the BDCCs

MIC of the BDCCs

The lowest concentration, which shows no growth of tested organism after macroscopic evaluation, was determined as the MIC.[16] Fig. 4 presents the MIC values of the 13 BDCCs against Sa and Ec.

The 13 BDCCs showed excellent antimicrobial activity toward Ec and Sa (Fig. 4). Except for **1b**, the MICs of the BDCC against Sa is equal to or less than that of natural capsaicin, which illustrates that these 12 BDCCs show antibacterial properties similar to or better than that of natural capsaicin. The poor inhibitory performance of **1b** may be attributed to its structure, which contains two *tert*-butyls

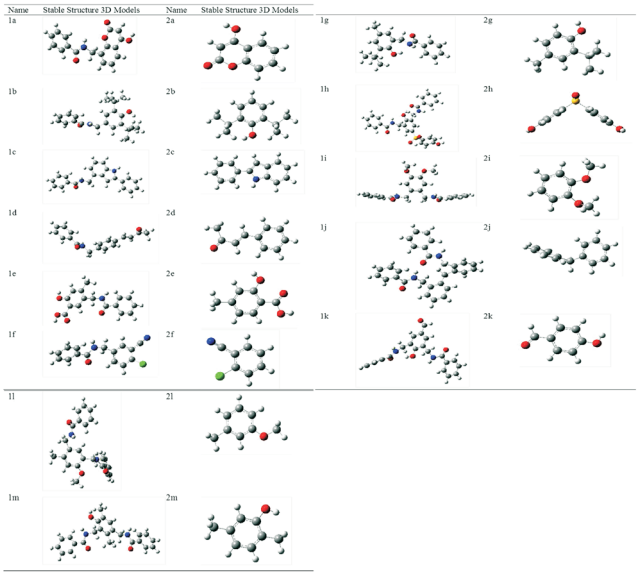

Fig. 3. Stable structure of monomers containing capsaicin.

and is sterically hindered. Thus, it is difficult to play bacteriostatic effect through the mechanism of bacterial bio-

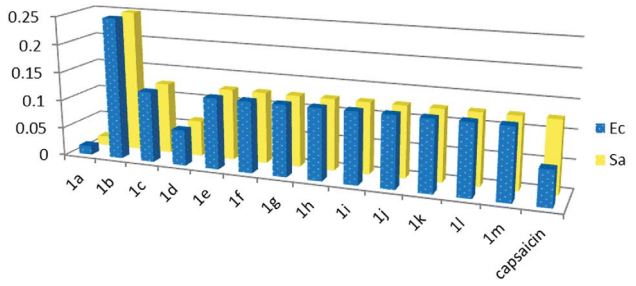

Fig. 4. MIC of thirteen tested compounds and capsaicin.

logical structures destroyed.[17]

The MICs of all of the BDCCs except **1a** against Ec are slightly larger than or equal to that of natural capsaicin, which indicates that they have relatively weak antibacterial properties. The improved antibacterial property of **1a** may be attributed to its heterocyclic structure, which endows the compound with a variety of biological activities and presents remarkable medicinal value and potential chemotherapeutic properties.[18] These advantages render **1a** with good activity against the two bacteria. Coupled with the compound containing a hydroxyl bond causes overall activity to increase, which easily exerts a bacteriostatic effect by destroying the bacterial biological structure.

As can be seen qualitatively, the quality of antibacterial properties is consistent with the $\Delta\varepsilon_{L\text{-}H}$ value and dipole of the quantum chemistry calculation, except for a few exceptions (see Fig. 4). Smaller $\Delta\varepsilon_{L\text{-}H}$ values of the compounds translate to greater activity and higher instability. More unstable compounds may lead to greater MIC, indicating poorer inhibition. From the perspective of the polarity of compounds, greater polarity indicates stronger hydrophilicity, and weaker hydrophobicity indicates weaker cell wall and cell membrane permeability. Therefore, greater polarities indicate poorer antibacterial activity.

Bacteriostatic ring results

Biocide additives were prepared in vitro to determine their microbial activity against Sa and Ec using the disc diffusion method (see Fig. 5). Table 2 reveals that the BDCCs show strong inhibitory effects against the tested bacteria, although **1b** presented inhibitory effects against Sa only. Each experiment was performed in triplicate, and the average value of three measurements was obtained. The diameters of bacteriostatic ring are shown in Table 2 (outer diameter of Oxford cup, 8 mm).

The diameters of the bacteriostatic ring are directly proportional to antimicrobial activity. All of the tested compounds present good antimicrobial activity, especially **1a**, **1f**, and **1l** (see Table 2). However, the antimicrobial activities of **1b**, **1i**, and **1g** are slightly poorer than those of others. Results of the analysis are consistent with our MIC findings.

Result of test panels in seawater

Biocide additives are commonly used to prolong the life of surface coatings. These additives prevent or slow the growth of organisms on the coating surface. Without biocide additives, biological species adhere to the coating surface, which can eventually lead to disbonding and blistering of coatings under various service conditions. The BDCCs were incorporated into paint coatings, and an experiment was performed at sea for 120 d, from June 2014 to September 2014, which is the period of vigorous growth of marine organisms (including marine algae, *Enteromorpha*, and barnacles). The results are shown in Fig. 6.

Macrofouling organisms, algae and microbial film, barnacles, and mussels are important marine organisms, and settlement of macrofouling organisms is based on formation of biofilms. We investigated the antifouling properties of the 13 new compounds by taking photographs of the test panels with surface attachment of marine organisms.

Biofouling is generally recognized to undergo two important stages.[19] The initial stage is formation of biological mucosa. Biological mucosa which is dominated by uniform particles of bacteria and diatoms forms on the surface of the immerged object. In certain antifouling coatings, this film presents stratified layers, which are divided into the bacterial and diatomic layers, and it sets the scene for later events.[20] The final stage of biofouling involves macro-

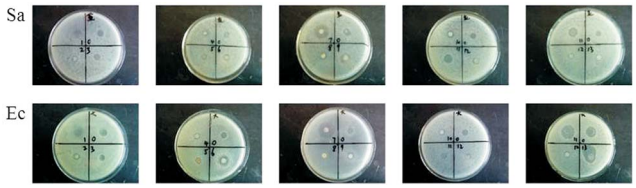

Fig. 5. Anti-microbial test specimens 1→**1a**, 2→**1i**, 3→**1b**, 4→**1j**, 5→**1c**, 6→**1h**, 7→**1k**, 8→**1d**, 9→**1e**, 10→**1f**, 11→**1g**, 12→**1l**, 13→**1m**, **O**→ acetone without tested compounds.

Table 2. The diameter of bacteriostatic rings

Compounds	**1a**	**1b**	**1c**	**1d**	**1e**	**1f**	**1g**	**1h**	**1i**	**1j**	**1k**	**1l**	**1m**	**O**
Sa/mm	14	10	10	12	13	13	10	11	10	10	12	13	12	8
Ec/mm	14	9	11	11	12	14	10	12	10	11	13	13	13	8

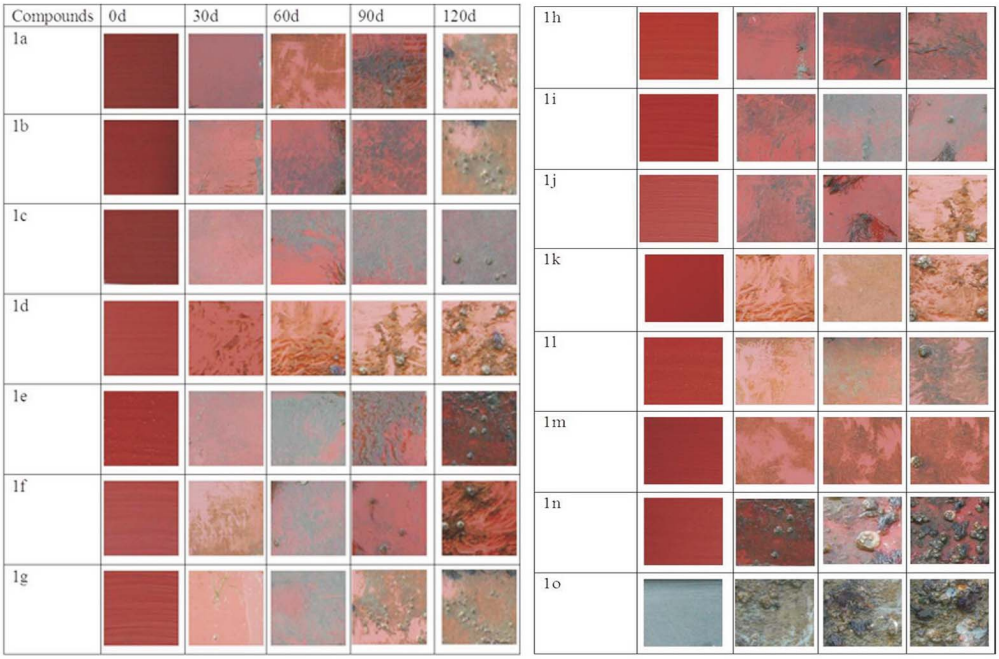

Fig. 6. Results of testing panels in the sea. Panel No.: (**1a**) 1343; (**1b**) 1344; (**1c**) 1345; (**1d**) 1346; (**1e**) 1347; (**1f**) 1348; (**1g**) 1349; (**1h**) 1350; (**1i**) 1351; (**1j**) 1352; (**1k**) 1353; (**1l**) 1354; (**1m**) 1355; (**1n**) 1342 the coating without capsaicin derivatives; (**1o**) blank.

organism accumulation. Spores of algae, marine fungi, and ciliate protozoa appear on the biofilm, and a more complex community is formed; these communities initiate settlement of other macroorganisms, such as mussels, barnacles, bryozoans, tubeworms, and algal growth.

The blank panel was covered with various biofilms and substantial green marine algae such as *Enteromorpha prolifera* (Fig. 6). No marine organisms were attached to the other panels at 30 day, except for panel 1342, which showed trace amounts of microbial mucosa. This result suggests that BDCCs as antifoulants can improve the antifouling properties of paint coatings. After 60 d, except for 1346 and 1345, which showed a small amount of algae and biofilms, other panels basically presented no microbial attachment. By contrast, 1342 and the blank panel showed small amounts of micro-organism mucosa and barnacles instead of *E. prolifera*; likely because of the unstable attachment of the bacteria to the panel. All other panels showed mud and a small quantity of microfilms. After 90 d, 1353, 1352, 1351, 1350, and 1349 also showed trace amounts of barnacle attachment; 1348, 1355, 1344, 1342, and the blank panel showed more attachment. Panel 1348 presented the best effect among the tested panels. Over a period of 120 d, certain biofilms and sludge in panels 1348, 1347 and 1355 were washed off by seawater. Most panels evidently exhibited biological mucosa and barnacles in comparison with the panels at 60 d, which indicates weakening of antifouling performance. More barnacles were found and attachment of barnacles occurred on the basis of biofilm on the panels. Panel 1348 showed some biofilm and barnacle formation. Panels 1343 to 1355 exhibited a certain degree of antifouling property, especially panels 1348, 1347, 1355, and 1354; these results indicate superior antifouling property in comparison with other panels.

We note that antifouling paints exhibiting BDCCs showed performance consistent with the $\Delta\varepsilon_{L\text{-}H}$ and dipole values of the experimental compounds with certain exceptions. Higher $\Delta\varepsilon_{L\text{-}H}$ values translate to lower activity of the compounds and better stability. Thus, the antifouling paints possess fairly long antifouling effect.

Adding BDCCs to paint can significantly improve antifouling performance, especially at the most vigorous period of barnacle growth. This study presents a new method for the future development of environment-friendly antifouling paints.

EXPERIMENTAL

General materials: 4-Hydroxycoumarin, 1,2-dimethoxy-

benzene, 2,6-di-*tert*-butylphenol, diphenylmethane, 2-phenylindole, 4,4'-sulfonyldiphenol, *p*-hydroxybenzaldehyde, benzalacetone, 4-methylsalicylic acid, 2-chlorobenzonitrile, 2-tert-butyl-4-methylphenol, 3-methylanisole, 2,5-dimethylphenol, and *N*-(hydroxymethyl)benzamide were purchased from Aladdin or local companies. All solvents used in the experiments were at least of reagent grade administered without further purification.

Synthesis of 13 BDCCs: Thirteen compounds were synthesized by Friedel-Crafts alkylation,[21,22] which requires Lewis and proton acids as catalysts. Taking **1a** as an example, (35.4 g, 0.2 mol) of *N*-(hydroxymethyl)benzamide, (16.2 g, 0.1 mol) of 4-hydroxycoumarin, and (50 mL) absolute ethanol were added to a 250 mL three-necked round-bottom flask in a heating water bath (35 °C) and then stirred. Concentrated sulfuric acid was then added to this solution in drops (reaction time: 5 d). The resultant white precipitate was recrystallized in ethanol and then dried under vacuum to obtain a white powder.

Characterization studies: The resultant monomers were characterized by ^{1}H and ^{13}C NMR, HRMS, IR, and elemental analysis. Thirteen benzamide derivatives containing capsaicin (BDCCs), which are respectively denoted as **1a**, **1b**, **1c**, **1d**, **1e**, **1f**, **1g**, **1h**, **1i**, **1j**, **1k**, **1l**, and **1m** (Fig. 7), were synthesized in our laboratory.

N-[(4-hydroxy-2-oxo-2*H*-chromen-8-yl)methyl]benzamid e (**1a**): white powder, yield: 83.3%, m.p. 221.8~222.6 °C. IR (KBr):/cm^{-1}: $\upsilon_{C\text{-}C}$ = 755.19, υ_{CH2} = 1563.20, $\upsilon_{C=C}$ = 1624.32, $\upsilon_{CO\text{-}N}$ = 1678.56, $\upsilon_{=CH}$ = 3062.76, υ_{OH} = 3330.05; ^{1}HNMR (DMSO-d$_6$, 600 MHz), δ(ppm): 4.403 (d, J = 5.4 Hz, 2H, CH_2), 7.399 (d, J = 6.0 Hz, 2H, PhH), 7.511 (t, J = 8.0 Hz, 2H, PhH), 7.602 (t, J = 7.4 Hz, 1H, PhH), 7.643 (s, 1H, HOCCHCO), 7.971 (d, J = 5.9 Hz, 3H, PhH), 9.859 (t, J = 5.9 Hz, 1H, NH), 13.154 (s, 1H, OH); ^{13}C NMR (150.9 MHz, DMSO-d_4): δ = 170.05, 164.06, 163.16, 152.93, 133.17, 132.76, 132.51, 128.98, 128.18, 124.63, 124.21, 116.67, 116.62, 102.39, 34.98; HRMS, *m/z*: 296.0909 ([M+H]$^+$), 318.0733 ([M+Na]$^+$); Elemental analysis (EA), $C_{17}H_{13}NO_4$: 295.2894, found(calculated), C:68.95%(69.15%), H:4.14% (4.44%), N: 5.00%(4.74%).

^{1}H and ^{13}C NMR data were consistent with the number and location of hydrogen and carbon, and all spectroscopic data were identical to the structure of the compound **1a**.

N-[(4-hydroxy-3, 5-di-*tert*-butyl) methyl)]benzamide (**1b**): white powder, yield 76.5%. m. p.: 195.3-196.0 °C. IR (KBr): /cm^{-1}: $\upsilon_{C\text{-}C}$ = 715.50, υ_{CH2} = 1539.55, $\upsilon_{CO\text{-}N}$ = 1635.76, $\upsilon_{C\text{-}H}$ = 2961.05, υ_{OH} = 3634.30; ^{1}H NMR (DMSO-d$_6$, 600 MHz), δ (ppm): 1.324 (s, 18H, $C(CH_3)_3$), 4.337 (d, J = 6.0 Hz , 2H, CH_2), 6.791 (s, 1H, PhH), 7.044 (d, J = 5.4 Hz, 2H, PhH), 7.427 (t, J = 6.0 Hz, 2H, PhH), 7.827 (d, J = 7.2 Hz, 2H, PhH), 7.839 (t, J = 5.9 Hz, 1H, NH), 8.877 (s, 1H, OH); ^{13}C NMR (150.9 MHz, DMSO-d_4): δ = 166.61, 153.16, 139.53, 135.16, 131.55, 130.96, 128.77, 127.64, 124.15, 43.35, 34.94, 30.82; HRMS, *m/z*: 340.2282 ([M+H]$^+$), 362.2103 ([M+Na]$^+$); EA, $C_{22}H_{29}NO_2$: 339.4711, found (calculated) C: 77.82% (77.84%), H: 8.38% (8.61%), N: 4.30%(4.13%).

^{1}H and ^{13}C NMR data were consistent with the number and location of hydrogen and carbon, and all spectroscopic data were identical to the structure of the compound **1b**.

N-[(2-phenyl-1*H*-indol-4-yl) methyl]benzamide (**1c**): red powder, yield 88.9%. m. p.: 225.9-226.8 °C. IR (KBr):/cm^{-1}: $\upsilon_{C\text{-}C}$ = 696.54, $\upsilon_{C=C}$ = 1449.46, $\upsilon_{CO\text{-}N}$ = 1638.46, $\upsilon_{C\text{-}N}$ = 3402.83; ^{1}H NMR (DMSO-d$_6$, 600 MHz), δ (ppm): 1.321 (d, J = 6.0 Hz, 2H, CH_2), 4.310 (s, 1H, CCHC), 6.322 (d, J = 7.2 Hz, 2H, PhH), 7.403 (t, J = 5.4 Hz, 12H, PhH), 7.957 (t, J = 1.2 Hz, 1H, NH), 11.027 (s, 1H, NH); ^{13}C NMR (150.9 MHz, DMSO-d_4): δ = 167.56, 165.02, 151.22, 148.58, 138.35, 132.07, 130.49, 127.73, 126.85, 125.63, 123.79, 110.67, 56.65, 35.95, 35.29, 35.15, 29.94; HRMS, *m/z*: 349.1300 ([M+Na]$^+$); EA, $C_{22}H_{18}N_2O$: 326.3911, found (calculated) C: 80.72% (80.96%), H: 5.43% (5.56%), N: 8.48% (8.58%).

^{1}H and ^{13}C NMR data were consistent with the number and location of hydrogen and carbon, and all spectroscopic data were identical to the structure of the compound **1c**.

N-{4-[(1*Z*)-3-oxobut-1-en-1-yl] benzyl}benzamide (**1d**): brown powder, yield 45.9%. m. p.: 154.8-156.0 °C. IR (KBr): /cm^{-1}: $\upsilon_{C\text{-}C}$ = 696.12, $\upsilon_{C=O}$ = 1529.36, $\upsilon_{CO\text{-}N}$ = 1636.92, $\upsilon_{=CH}$ = 3058.83, υ_{OH} = 3440.49; ^{1}H NMR (DMSO-d$_6$, 600 MHz), δ (ppm): 4.882 (d, J = 5.4 Hz, 2H,CH_2), 5.237 (s, 3H, CH_3), 7.551 (d, J = 5.4 Hz, 8H, PhH), 7.924 (t, J = 7.2 Hz, 3H, PhH), 9.057 (t, J = 5.9 Hz, 1H, NH); ^{13}C NMR (150.9 MHz, DMSO-d_4): δ = 166.92, 134.42, 131.87, 129.73, 128.72, 127.89, 45.64; HRMS,

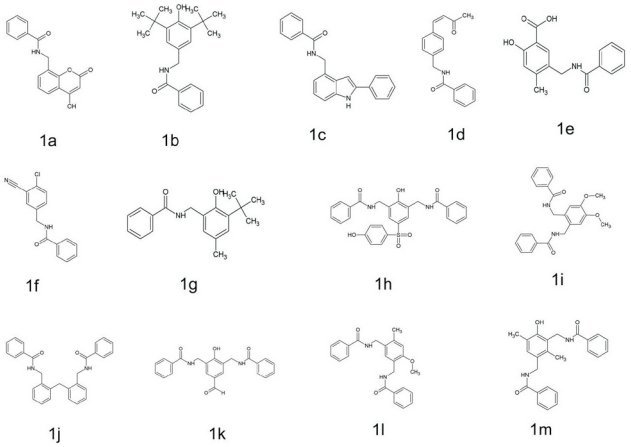

Fig. 7. Structures of 13 BDCCs.

m/z: 280.1335 ($[M+H]^+$), 302.1157 ($[M+Na]^+$); EA, $C_{18}H_{17}NO_2$: 279.3330, found (calculated) C: 77.71% (77.40%), H: 5.82% (6.13%), N: 5.39% (5.01%).

^1H and ^{13}C NMR data were consistent with the number and location of hydrogen and carbon, and all spectroscopic data were identical to the structure of the compound **1d**.

N-(2-methyl-4-hydroxyl-5-carboxyl)benzamide (**1e**): white powder, yield 59.7%. m. p.: 135.6-136.2 °C. IR (KBr): /cm^{-1}: υ_{C-C} = 694.26, υ_{CH3} = 1286.57, υ_{COOH} = 1527.48, υ_{CO-N} = 1635.30, υ_{OH} = 3307.23; ^1H NMR (DMSO-d_6, 600 MHz), δ (ppm): 2.338 (d, J = 2.7 Hz, 2H, CH_2), 3.831 (s, 3H, CH_3), 6.870 (s, 1H, PhH), 7.473 (t, J = 7.8 Hz, 3H, PhH), 7.544 (d, J = 7.2Hz, 2H, PhH), 7.644 (t, J = 6.0Hz, 1H, PhH), 7.690 (t, J = 7.8 Hz, 1H, NH), 7.913 (s, 1H, OH), 9.041 (s, 1H, COOH); ^{13}C NMR (150.9 MHz, DMSO-d_4): δ = 166.92, 134.42, 131.87, 128.72, 127.89, 127.71, 120.81, 117.64, 45.64; HRMS, *m/z*: 286.1077 ($[M+H]^+$), 308.0898 ($[M+Na]^+$); EA, $C_{16}H_{15}NO_4$: 285.2946, found (calculated) C: 67.08% (67.36%), H: 5.63% (5.30%), N: 4.97% (4.91%).

^1H and ^{13}C NMR data were consistent with the number and location of hydrogen and carbon, and all spectroscopic data were identical to the structure of the compound **1e**.

N-(4-chloro-3-cyanobenzyl)benzamide (**1f**): white powder, yield 35.9%. m. p.: 130.8-132.1 °C. IR (KBr):/cm^{-1}: υ_{C-Cl} = 694.23, υ_{C-C} = 1287.69, $\upsilon_{C=O}$ = 1527.86, υ_{CO-N} = 1635.55; ^1H NMR (DMSO-d_6, 600 MHz), δ (ppm): 4.867 (d, J = 6.0 Hz, 2H, CH_2), 7.031 (s, 1H, PhH), 7.116 (d, J = 9.0 Hz, 1H, PhH), 7.463 (d, J = 8.4 Hz, 2H, PhH), 7.521 (t, J = 1.2 Hz, 1H, PhH), 7.905 (t, J = 7.2 Hz, 3H, PhH), 9.037 (t, J = 5.9 Hz, 1H, NH); ^{13}C NMR (150.9 MHz, DMSO-d_4): δ = 166.93, 134.41, 133.35, 131.88, 129.73, 129.05, 128.73, 127.88, 45.65; HRMS, *m/z*: 293.0689 ($[M+Na]^+$); EA, $C_{15}H_{11}ClN_2O$: 270.7136, found (calculated) C: 66.49% (66.55%), H: 4.53% (4.10%), N: 10.09% (10.35%).

^1H and ^{13}C NMR data were consistent with the number and location of hydrogen and carbon, and all spectroscopic data were identical to the structure of the compound **1f**.

N-(3-*tert*-butyl-2-hydroxy-5-methylbenzyl)benzamide (**1g**): white crystal, yield 58.8%. m.p.: 162.5-163.4 °C. IR (KBr) $\tilde{\nu}$/cm^{-1}: υ_{C-C} = 735.72, υ_{CH3} = 1549.48, υ_{CO-N} = 1608.10, υ_{C-H} = 3082.78, υ_{OH} = 3327.52; ^1H NMR (DMSO-d_6, 600 MHz), δ (ppm): 1.347 (s, 9H, $C(CH_3)$), 2.186 (s, 3H, CH_3), 4.362 (d, J = 6.0 Hz, 2H, CH_2), 6.926 (d, J = 1.8 Hz, 2H, PhH), 7.502 (t, J = 7.8 Hz, 2H, PhH), 7.563 (s, 1H, PhH), 7.911 (d, J = 0.9 Hz, 2H, PhH), 9.489 (t, J = 5.9 Hz, 1H, NH), 9.573 (s, 1H, OH); ^{13}C NMR (150.9 MHz, DMSO-d_4): δ = 168.43, 151.99, 137.55, 133.30, 132.38, 129.13, 128.99, 127.86, 127.69, 127.11, 126.50, 34.88, 30.12, 20.99; HRMS, *m/z*: 298.1808 ($[M+H]^+$), 320.1629 ($[M+Na]^+$); EA, $C_{19}H_{23}NO_2$: 297.3914, found (calculated) C: 76.88% (76.73%), H: 7.71% (7.80%), N: 4.88% (4.71%).

^1H and ^{13}C NMR data were consistent with the number and location of hydrogen and carbon, and all spectroscopic data were identical to the structure of the compound **1g**.

N-{2-hydroxy-3-methylbenzamide-5-[(4-hydroxyphenyl) sulfonyl]benzyl}benzamide (**1h**): yellow powder, yield 29.6%. m. p.: 131.6-132.9 °C. IR (KBr):/cm^{-1}: υ_{C-C} = 693.73, $\upsilon_{S=O}$ = 1286.73, υ_{CO-N} = 1635.86, υ_{OH} = 3308.95; ^1H NMR (DMSO-d_6, 600 MHz), δ (ppm): 4.872 (d, J = 6.0 Hz, 2H, CH_2), 5.675 (d, J = 3.3 Hz, 4H, PhH), 6.903 (d, J = 9.0 Hz, 2H, PhH), 7.468 (t, J = 7.8 Hz, 4H, PhH), 7.526 (d, J = 7.8 Hz, 2H, PhH), 7. 630 (s, 2H, PhH), 7.878 (t, J = 7.2 Hz, 4H, PhH), 7.899 (t, J = 5.9 Hz, 2H, NH), 9.038 (s, 2H,OH); ^{13}C NMR (150.9 MHz, DMSO-d_4): δ = 166.94, 162.06, 134.41, 132.55, 131.88, 129.81, 128.73, 127.89, 116.42, 45.66; HRMS, *m/z*: 517.1433 ($[M+H]^+$), 539.1258 ($[M+Na]^+$); EA, $C_{28}H_{24}N_2O_6S$: 516.5649, found (calculated) C: 65.29% (65.10%), H: 4.68% (4.68%), N: 5.08% (5.42%).

^1H and ^{13}C NMR data were consistent with the number and location of hydrogen and carbon, and all spectroscopic data were identical to the structure of the compound **1h**.

N-(2-methylbenzamide-4, 5-dimethoxybenzyl)benzamide (**1i**): white powder, yield 59.8%. m. p.: 192.7-193.3 °C. IR (KBr):/cm^{-1}: υ_{C-C} = 692.35, υ_{CH3-O} = 1274.54, υ_{CO-N} = 1627.92; ^1H NMR (DMSO-d_6, 600 MHz), δ (ppm): 3.699 (s, 6H, OCH_3), 4.532 (d, J = 5.4 Hz, 4H, CH_2), 6.952 (s, 2H, PhH), 7.464 (t, J = 7.2 Hz, 4H, PhH), 7.517 (d, J = 6.0 Hz, 2H, PhH), 7. 884 (t, J = 7.2 Hz, 4H, PhH), 8.938 (t, J = 5.4 Hz, 2H, NH); ^{13}C NMR (150.9 MHz, DMSO-d_4): δ = 166.58, 148.18, 134.80, 131.69, 129.78, 128.78, 127.71, 113.43, 56.09; HRMS, *m/z*: 405.1807 ($[M+H]^+$), 427.1629 ($[M+Na]^+$); EA, $C_{24}H_{24}N_2O_4$: 404.4583, found (calculated) C: 71.60% (71.27%), H: 6.28% (5.98%), N: 7.13% (6.93%).

^1H and ^{13}C NMR data were consistent with the number and location of hydrogen and carbon, and all spectroscopic data were identical to the structure of the compound **1i**.

(2, 2'-bis-benzamide methyl)diphenyl methane (**1j**): white powder, yield 64.4%. m. p.: 201.7-202.6 °C. IR (KBr):/cm^{-1}: υ_{C-C} = 694.26, υ_{CH2} = 1528.03, υ_{CO-N} = 1635.99; ^1H NMR (DMSO-d_6, 600 MHz), δ (ppm): 3.933 (s, 4H, CH_2), 6.132 (d, J = 5.4 Hz, 4H, PhH), 6.881 (t, J = 5.4 Hz, 2H, PhH), 7.093 (d, J = 3.0 Hz, 4H, PhH), 7.230 (d, J = 7.2 Hz, 4H, PhH), 7.293 (t, J = 7.8 Hz, 2H, PhH), 7.914 (t, J = 7.2 Hz, 4H, PhH), 9.047 (t, J = 5.4 Hz, 2H, NH); ^{13}C NMR (150.9 MHz, DMSO-d_4): δ = 166.93, 134.42, 131.88, 128.73, 127.89, 45.65; HRMS, *m/z*: 457.1883 ($[M+Na]^+$); EA, $C_{29}H_{26}N_2O_2$: 434.5289, found (calculated) C: 80.58% (80.16%%), H: 6.44% (6.03%), N: 6.66% (6.45%).

^{1}H and ^{13}C NMR data were consistent with the number and location of hydrogen and carbon, and all spectroscopic data were identical to the structure of the compound **1j**.

N, *N*′-[(5-formyl-2-hydroxy-1, 3-phenylene)bis(methylene)]dibenzamide (**1k**): white powder, yield 41.2%. m. p.: 198.5-199.5 °C. IR (KBr):/cm^{-1}: $\upsilon_{C\text{-}C}$ = 694.08, $\upsilon_{CO\text{-}H}$ = 1527.46, $\upsilon_{CO\text{-}N}$ = 1634.68, υ_{OH} = 3307.88; ^{1}H NMR (DMSO-d$_6$, 600 MHz), δ (ppm): 4.197 (s, 4H, CH_2), 5.879 (d, J = 5.4 Hz, 4H, PhH), 7.482 (t, J = 7.2 Hz, 2H, PhH), 7.526 (s, 2H, PhH), 7.553 (t, J = 7.2 Hz, 4H, PhH), 7.910 (t, J = 7.8 Hz, 2H, NH), 7.922 (s, 1H, OH), 9.046 (s, 1H, CHO); ^{13}C NMR (150.9 MHz, DMSO-d_4): δ = 166.93, 134.42, 131.88, 129.73, 129.04, 128.73, 127.89, 45.65; HRMS, *m/z*: 411.1317 ([M+Na]$^+$); EA, $C_{23}H_{20}N_2O_4$: 388.4159, found (calculated) C: 70.96% (71.12%), H: 5.66% (5.19%), N: 7.75% (7.21%).

^{1}H and ^{13}C NMR data were consistent with the number and location of hydrogen and carbon, and all spectroscopic data were identical to the structure of the compound **1k**.

N-(4-methoxy-5-methylbenzamide-2-methylbenzyl)benza mide (**1l**): white powder, yield 50.3%. m. p.: 190.6-191.1 °C. IR (KBr):/cm^{-1}: $\upsilon_{C\text{-}C}$ = 692.98, $\upsilon_{CH3\text{-}O}$ = 1256.34, υ_{CH3} = 1547.69, $\upsilon_{CO\text{-}N}$ = 1642.04; ^{1}H NMR (DMSO-d$_6$, 600 MHz), δ (ppm): 2.313 (s, 3H, CH_3), 3.805 (s, 3H, OCH_3), 4.397 (d, J = 6.0 Hz, 4H, CH_2), 6.822 (s, 1H, PhH), 7.145 (s, 1H, PhH), 7.396 (t, J = 8.4 Hz, 4H, PhH), 7.496 (d, J = 8.4 Hz, 2H, PhH), 7.777 (d, J = 7.2 Hz, 4H, PhH), 8.801 (t, J = 6.0 Hz, 2H, NH); ^{13}C NMR (150.9 MHz, DMSO-d_4): δ = 166.83, 166.63, 155.68, 135.43, 135.06, 131.43, 129.21, 128.60, 127.67, 126.99, 124.54, 112.77, 55.92, 37.69, 19.29; HRMS, *m/z*: 389.1862([M+H]$^+$), 411.1687 ([M+Na]$^+$); EA, $C_{24}H_{24}N_2O_3$: 388.4589, found (calculated) C: 74.15% (74.21%), H: 6.34% (6.23%), N: 7.21% (7.21%).

^{1}H and ^{13}C NMR data were consistent with the number and location of hydrogen and carbon, and all spectroscopic data were identical to the structure of the compound **1l**.

N-(4-hydroxy-3-methylbenzamide-2, 5-dimethylbenzyl) benzamide (**1m**): white crystal, yield 20.6%. m. p.: 201.2-202.1 °C. IR (KBr):/cm^{-1}: $\upsilon_{C\text{-}C}$ = 710.48, υ_{CH3} = 1303.70, $\upsilon_{CO\text{-}N}$ = 1636.08, υ_{OH} = 3264.21; ^{1}H NMR (DMSO-d$_6$, 600 MHz), δ (ppm): 2.138 (s, 3H, CH_3), 2.370 (s, 3H, CH_3), 4.406 (d, J = 6.0 Hz, 2H, CH_2), 4.477 (d, J = 5.4 Hz, 2H, CH_2), 7.023 (s, 1H, PhH), 7.543 (d J = 5.4 Hz, 4H, PhH), 7.567 (t, J = 7.8 Hz, 1H, PhH), 7.913 (t, J = 7.8Hz, 4H, PhH), 8.716 (d, J = 7.2 Hz, 1H, PhH), 9.395 (t, J = 6.0 Hz, 2H, NH), 9.970 (s,1H, OH); ^{13}C NMR (150.9 MHz, DMSO-d_4): δ = 169.05, 166.33, 153.75, 134.93, 134.38, 133.42, 132.31, 131.55, 131.11, 128.86, 128.68, 128.28, 128.01, 127.77, 124.19, 122.71, 41.89, 37, 05, 16.84, 15.22; HRMS, *m/z*: 389.1863 ([M+H]$^+$), 411.1684 ([M+Na]$^+$); EA, $C_{24}H_{24}N_2O_3$: 388.4589, found (calculated) C: 74.01% (74.21%), H: 6.36% (6.23%), N: 7.40% (7.21%).

^{1}H and ^{13}C NMR data were consistent with the number and location of hydrogen and carbon, and all spectroscopic data were identical to the structure of the compound **1m**.

Therefore, all characterization results were in agreement with the proposed structures of the products. The results of spectrum are shown in the Supporting Information.

Quantum chemistry studies

To achieve better insights into the molecular structure of BDCCs, quantum chemical analysis was performed using Gaussian 3, a program that is routinely used to investigate chemical structures, polymeric systems, and types of biological activity. The most stable conformer for the compounds was fully geometrical optimized by molecular orbital theory.[23] Computational studies for compound property prediction were performed by determination of several parameters.

Antimicrobial screening: The antimicrobial activity of the synthesized compounds was tested against *Staphylococcus aureus* (Sa; Gram-positive bacteria, ATCC 13565) and *Escherichia coli* (Ec; Gram-negative bacteria, ATCC 12435), both of which were provided by the Laboratory of Microorganisms at the Ocean University of China. The bacteria were cultivated in a biochemical incubator and prepared for the experiments. Nutrient agar was used as a medium.

Antibacterial activity test

Bacterial activation: Sa and Ec were respectively inoculated on basal medium (peptone, 5.0 g; beef extract, 1.5 g; NaCl, 2.5 g; distilled water, 500 mL; pH = 7.2, 10 min of sterilization at 121 °C) kept in a refrigerator,[24] activated for 24 h at 37 ± 1 °C. A single bacterial colony was obtained from this culture. Bacteria were scraped from the culture plate and resuspended in 5 mL of liquid nutrient medium to obtain the desired final concentration of 10-fold serial dilutions.

Minimum inhibitory concentration (MIC) test for determination of antimicrobial activity

The resistance or sensitivity of a bacterial species can simply be assessed by direct comparison of its MIC with the concentrations of the agent that can be expected in the environment. In this work, the 2-fold serial dilution method was used.[25] First, 2 mL of nutrient fluid medium was added to test tubes using a pipette. The initial concentration of each test compound was 1 mg/mL (solvent, acetone), doubling dilution in turns followed by vortex mixing.[26] Two control groups, one with the bacterial inoculate but without the tested compounds and a group without the bacterial inoculate or tested compounds, were established. Exact bacterial concentrations were obtained (105 cfu/mL; cfu, co-

lony-forming unit: colony formed on the agar plate after cultivation) by 10-fold dilution. Finally, Sa and Ec at the exponential growth phase were incubated with increasing doses of each of the thirteen tested compounds (range, 0–1 mg/mL) at 37 °C for 24 h in liquid nutrient medium. An ultraviolet spectrophotometer was used to determine the MIC of each compound.

All experimental procedures were completed in the purification table, and each experiment was performed in triplicate. During MIC determinations, the term inhibition refers to total loss of ability to multiply.

Agar diffusion method for antimicrobial activity determination

The agar diffusion method is used to determine what antibiotics/compounds, inhibit bacterial growth or alternatively are bacteriostatic. The agar was soaked with a selected antibiotic/chemical and then placed on a lawn of bacteria in a Petri dish. Inhibition zones were measured around an Oxford cup to determine whether or not the bacteria are resistant or susceptible to the selected antibiotic/chemical. Sterilized medium with bacterial suspension (105 cfu/ mL) was poured onto a Petri dish to a depth of 3–4 mm. An Oxford cup impregnated with the test compounds (solvent, acetone) was placed on the solidified medium; this setup was incubated at 37 °C for 24 h to study antibacterial and antifungal activities. A group without the tested compounds was used as a control.

Antifouling properties of BDCCs: To develop new antifouling paints, testing and quantifying the efficiency of new antifoulants is crucial. However, all previously reported methods are characterized by a lack of precise assessment of paint performance.[27]

Therefore, we considered the BDCCs as an auxiliary material (antifoulant) added to commonly used antifouling paints. The performance of the BDCCs in antifouling paints was observed and compared with the performance of antifouling paint without capsaicin derivatives and a blank according to GB 5370-85.[28]

We polished and descaled PVC panels (900 mm × 300 mm × 3 mm) with sandpaper so that the antifouling paints adhere to the substrate more easily and divided it into several parts. Antifouling coatings containing the thirteen new compounds were prepared according to Table 3 and then brushed three times onto the panels, which were then fastened in air and dried. The test panels were immersed in the waters of two ports in Qingdao, China, to a depth of 1.5 m for a period of 120 d and inspected and photographed at regular intervals. Thirteen new compounds and two controls (i.e., paint without BDCCs and a blank) were tested.

Table 3. Composition of antifouling coatings (g)

Panel No.	Acrylic resin	Cuprous oxide	Pigment	Antifoulant	Assistant	Xylene
1343	55	25	17	**1a**	2	11
1344	55	25	17	**1b**	2	11
1345	55	25	17	**1c**	2	11
1346	55	25	17	**1d**	2	11
1347	55	25	17	**1e**	2	11
1348	55	25	17	**1f**	2	11
1349	55	25	17	**1g**	2	11
1350	55	25	17	**1h**	2	11
1351	55	25	17	**1i**	2	11
1352	55	25	17	**1j**	2	11
1353	55	25	17	**1k**	2	11
1354	55	25	17	**1l**	2	11
1355	55	25	17	**1m**	2	11
1342	55	25	17	**1n**	2	11
blank	0	0	0	**1o**	0	0

CONCLUSIONS

Thirteen new benzamide derivatives were successfully synthesized through Friedel-Crafts alkylation from N-(hydroxylmethyl) benzamide and aromatic hydrocarbon-derived compounds. Three parameters, namely, $\Delta\varepsilon_{L\text{-}H}$, HF values, and dipole, were also obtained by quantum chemical calculation. The relationship between the three parameters and properties such as activity, stability, and polarity was discussed. Results suggest that the orders of $\Delta\varepsilon_{L\text{-}H}$ and dipole are consistent with the antimicrobial and antifouling performance of the resultant products. The antibacterial activity of the BDCCs was evaluated by MIC and bacteriostatic ring tests. The BDCCs were used as antifoulant coatings on panels to examine their antifouling performance over four months in sea. The experimental results demonstrated the excellent antifouling performance of all BDCCs.

Therefore, compounds containing the active capsaicin structure present good application prospects in environment-friendly antifouling coatings.

ACKNOWLEDGEMENTS

The authors gratefully acknowledge financial support by National Ocean Public Welfare Projects of China (No. 201005028-2), National Science and Technology Support Program of China (No. 2012BAB15B02), and National Natural Science Foundation of China (No. 50673085).

REFERENCES

1. Almeida, E.; Diamantine, T. C.; de Sousa, O. *Prog. Org.*

Coat. **2007**, *59*, 2-20.
2. Chambers, L. D.; Stokes, K. R.; Walsh, F. C.; Wood, R. J. K. *Surf. Coat. Tech.* **2006**, *201*, 3642-3652.
3. Motley, J. *Pestici. Biochem. Physiol.* **1978**, *9*, 340-345.
4. Hoch, M. *Appl. Geochem.* **2001**, *16*, 719-743.
5. Dowson, P. H.; Bubb, J. M.; Lester, J. N. *Mar. Pollut. Bull.* **1993**, *26*, 487-494.
6. Axiak, V.; Vella, A. J.; Agius, D.; Bonnici, P.; Cassar, G.; Cassone, R.; Chircop, P.; Micallef, D.; Mintoff, B.; Sammut, M. *Sci. Total Environ.* **2000**, *258*, 89-97.
7. Negri, A. P.; Hales, L. T.; Battershill, C.; Wolff, C.; Webster, N. S. *Mar. Pollut. Bull.* **2004**, *48*, 1142-1144.
8. Yebra, D. M.; Kiil, S.; Dam-Johansen, K. *Prog. Org. Coat.* **2004**, *50*, 75-104.
9. Evans, S. M.; Birchenough, A. C.; Brabcato, M. S. *Mar. Pollut. Bull.* **2000**, *40*, 204-211.
10. Clare, A. *New Sci.* **1995**, *145*, 38.
11. Fischer, K. J. US 5226380, 1993.
12. Watts, J. L. US 5397385, 1995.
13. Bullat, D. M.; Vasishtha, N. US 5925370, 1999.
14. Ravi, P. S.; Rajesh, M. K.; Kusum, L. C.; Saravanan, P.; Singh, V. K. *Tetrahedron* **2001**, *57*, 241-247.
15. John, E. C.; Kan, N. *Adv. Environ. Res.* **2000**, *4*, 307-312.
16. Pernak, J.; Skrzypczak, A. *Eur. J. Med. Chem.* **1996**, *31*, 901-903.
17. Cong, W.-W.; Yu, L.-M. *Chem. Res. Chin. U.* **2011**, *27*, 803-807.
18. Abd El-Wahab, H.; Abd El-Fattah, M.; Abd El-Khalik, N.; Nassar, H. S.; Abdelall, M. M. *Prog. Org. Coat.* **2014**, *77*, 1506-1511.
19. Dobretsov, S.; Dahms, H. U.; Qian, P. Y. *Biofouling* **2006**, *22*, 43-54.
20. Abarzua, S.; Jakubowski, S.; Eckert, S. *Bot. Mar.* **1999**, *42*, 459-465.
21. Lele, B. S.; Gore, M. A.; Kulkarni, M. G. *J. Appl. Polym. Sci.* **1999**, *73*, 1845-1850.
22. Friedel, C.; Crafts, J. M. *Compt. Rend.* **1877**, *84*, 1392-1450.
23. Stewart, J. J. P. *MOPAC Manual*, 7th ed.; Stewart Computational Chemistry: Paddington Circle, Colorado Springs, CO, USA, 1993.
24. Chen, F. S.; Xu, Y. P. CN 101045909, 2007.
25. Muraina, I. A.; Picard, J.; Eloff, J. N. *Phytomedicine* **2009**, *16*, 262-264.
26. Alderman, D.; Smith, P. *Aquaculture* **2001**, *196*, 211-243.
27. Mittelman, M. W.; Packard, J.; Arrage, A. A. *J. Microbiol. Meth.* **1993**, *18*, 51-60.
28. GB/T 5370-85, Antifouling Panels in Shallow Submergence, State Bureau of Standards, 1985.

